Elastic properties of polymer composites reinforced with C_{60} fullerene and carbon onion: Molecular dynamics simulation

Razie Izadi, Esmaeal Ghavanloo*, Ali Nayebi

School of Mechanical Engineering, Shiraz University, Shiraz 71963-16548, Iran

Abstract

In this paper, the elastic properties of polymer nanocomposites reinforced with C_{60} fullerene and $C_{60}@C_{240}$ carbon onion are estimated by using a molecular dynamic (MD) simulation. The nanocomposites are constructed by embedding the buckminsterfullerene and the carbon onion into an amorphous polymer matrix with different weight fractions. The poly methyl methacrylate (PMMA) is chosen as the polymer matrix. The results demonstrate that Young's modulus of the composite increases with increasing the weight fractions of the nanoscopic additives, which is consistent with experimental observations. The nanocomposite containing 4 wt.% of C_{60} exhibits Young's modulus of 3.774 GPa that is 24% higher than pure PMMA. In addition, the validity of the present simulation is verified by comparison with the experimental results.

Keywords: Molecular dynamics simulation; Nanocomposite; Fullerene; Carbon onion; Elastic property

1. Introduction

Polymer materials reinforced with nanoscopic structures have recently received considerable attention in both scientific and industrial communities [1]. Carbon-based nanoscopic structures such as carbon nanotubes and graphene sheets have been widely used as a reinforcement of polymer composites [2]. In recent years, experimental evidences show that, by incorporating fullerene molecules and their derivatives into the polymeric matrices, new generation of isotropic-like nanocomposites have been developed [3, 4]. Furthermore, it was shown that the spherical fullerene molecules are nearly size-independent reinforcements [5]. However, compared to the mechanical properties of polymer composites reinforced with the carbon nanotubes and graphene sheets, the elastic properties of the fullerene reinforced polymer composites (FRPC) are much less studied.

* Corresponding author.

Tel.: +98-7136133251, Fax: +98 7136473511

E-mail: ghavanloo@shirazu.ac.ir (E. Ghavanloo)

The first attempt to study the mechanical properties of the FRPC was made by Adnan and co-workers [6, 7]. Based on the molecular dynamics (MD) simulations, they investigate the influence of filler size on the elastic properties of the FRPC. However, the fullerenes were modelled via non-deformable solid inclusions in their simulations. Ogasawara et al. [8] experimentally studied the influence of fullerene dispersion on the mechanical properties of carbon-fiber reinforced epoxy matrix composites. In another study, the influence of fullerene fillers on the mechanical properties of nanocomposites with two different polymer matrices was investigated [9]. Hashemi Gahruei [10] developed several finite element models to predict the mechanical properties of polymer composites reinforced with fullerene molecules. The MD simulation study was performed to show the effects of fullerene fillers on the thermo-elastic properties of Araldite LY 5052/Aradur HY 5052 cross-linked resin epoxy [11]. Furthermore, the elastic properties of high density polyethylene reinforced by the graphene sheet and the fullerene molecules was estimated by the MD simulation [5]. Recently, Giannopoulos and co-workers [12] proposed a combined MD simulation and finite element method for the prediction of the elastic properties of the FRPC. By reviewing the mentioned studies, it can be concluded that the elastic properties of the fullerene/poly methyl methacrylate (PMMA) and carbon onion/PMMA composites have not been determined so far.

In view of the above remarks, we have pursued two main objectives in this paper:

1) The estimation of the elastic properties of C_{60}/PMMA by using the MD simulation. The choice of PMMA as the polymer matrix is due to the fact that it is widely used in various applications for its many advantageous properties.
2) The estimation of the the elastic properties of carbon onion reinforced polymer composites for the first time in the literature.

In this connection, we use the Materials Studio software to conduct the MD simulation. To model the interactions among nanofillers and polymers atoms, the Condensed Phase Optimized Molecular Potential for Atomistic Simulation Studies (COMPASS) is employed. In the present study, the elastic constants are calculated by the Voigt-Reuss-Hill approach. The effect of the weight fraction of C_{60} and $C_{60}@C_{240}$ molecules on the Young modulus and Poisson's ration of the composites is studied. The pure polymer matrix is also simulated to lead to better understanding the effect of nanofillers. In addition, the results obtained from the present simulation are compared with available experimental data. Our results can shed some lights on the application of this new type of composite. The organization of this paper is as follows. In Section 2, details of the MD simulation is discussed. Calculation of effective elastic constants by

using the Voigt-Reuss-Hill approach is discussed in Section 3. The numerical results are given in Section 4. Finally, summary and concluding remarks are presented in Section 5.

2. Molecular simulation

In this work, we use the Materials Studio software to perform the MD simulations. In addition, the Condensed Phase Optimized Molecular Potential for Atomistic Simulation Studies (COMPASS) is employed to model the interactions among fullerene and polymers atoms. It has been shown that the COMPASS force field is effective and accurate in handling polymer subjects in condensed [13]. All simulations are performed using a time step of 1 fs and a potential cutoff of 1.5 nm. In addition, the Nose-Hoover thermostat and the Berendsen barostat are used respectively for the system temperature and pressure conversion. Furthermore, to replicate the cells in three directions, periodic boundary conditions are imposed. To construct the molecular models of the nanocomposites, a nanofiller molecule (C_{60} or $C_{60}@C_{240}$) is placed in the center of a cubic representative volume elements (RVE). Then, PMMA molecules with 10 monomers (Fig. 1) are dispersed uniformly within the RVE in non-overlapping positions. The initial configuration of the RVE is constructed using the Amorphous Builder Module available in the Materials Studio, which builds molecules in a Monte Carlo fashion. The initial configuration of the RVE with 3 wt.% of C_{60} is shown in Fig. 2.

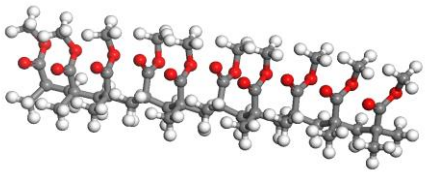

Fig. 1. Molecular structure of the PMMA polymer chain with 10 monomers

To achieve the minimum energy configuration of the RVE, we use the smart algorithm which is a cascade of the steepest descent, adjusted basis set Newton-Raphson, and quasi-Newton methods. Once the minimization process is completed, the temperature of the RVE increases above the glass transition temperature. Since the glass temperature of fullerene/PMMA is reported in the range of 358-364 K [14], the temperature of the RVE is increased to 500 K under constant volume for 50 ps. The model is then subjected to *NVT* ensemble for 250 ps at 500 K by keeping the cell dimensions fixed. Then, the RVE is put into an *NPT* ensemble with a pressure of 1 atm. and temperature of 500

K for 500 ps. The fluctuations of the density of the PMMA reinforced with 3 wt.% of C_{60} with respect to simulation time is shown in Fig. 3.

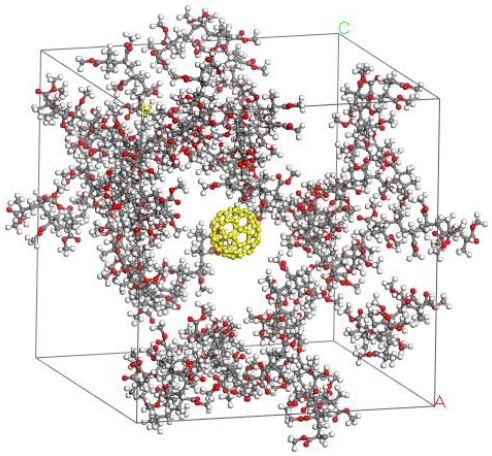

Fig. 2. Molecular unit cell model of PMMA reinforced with 3 wt.% of C_{60}.

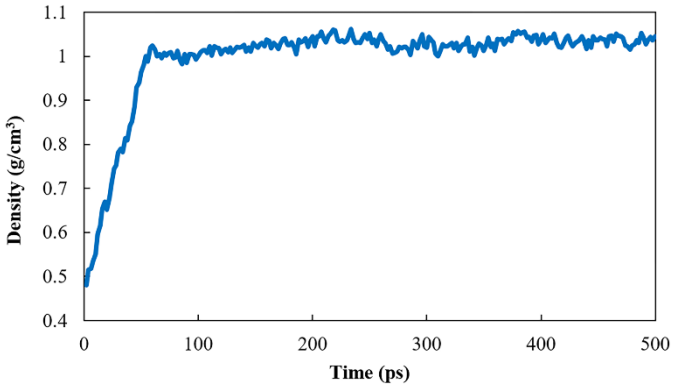

Fig. 3. Fluctuations of the density during *NPT* dynamics for external pressure of 1 atm. and temperature of 500 K.

After that, the system is cooled down to 298 K under constant pressure 1 atm. Finally, in order to equilibrate the RVE under ambient temperature and pressure, it is subjected to the *NPT* ensemble with a pressure 1 atm. and temperature of 298 K for 500 ps. Figure 4 shows the typical fluctuations in density of the RVE with 3 wt.% of C_{60}. It is observed that that the density of RVE quickly equilibrates in less than 40 ps and then continues to fluctuate around the equilibrium value. Figure 5 illustrates the final configuration of the PMMA reinforced with 3 wt.% of C_{60}. In addition, the initial and final characteristics of the RVEs with various concentration of C_{60} and $C_{60}@C_{240}$ are listed in Table 1. After aforementioned process, the RVE is suitable for calculating the elastic properties.

After the construction of the RVEs, the constant strain method, which was proposed by Theodorou and Suter [15], is used to calculate the elastic properties of the nanocomposites. In this method, the deformation of the RVE under uniaxial tension/compression and pure shear strains is studied statically.

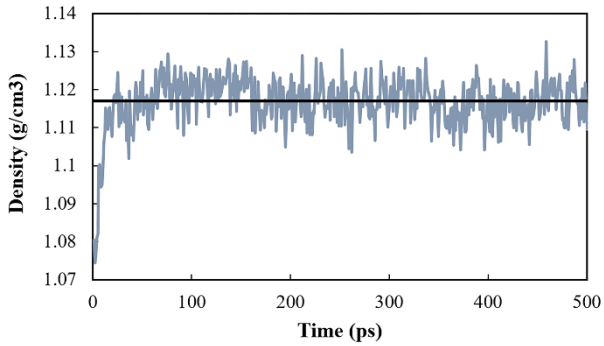

Fig. 4. Fluctuations of density during NPT dynamics for external pressure of 1 atm. and temperature of 298 K.

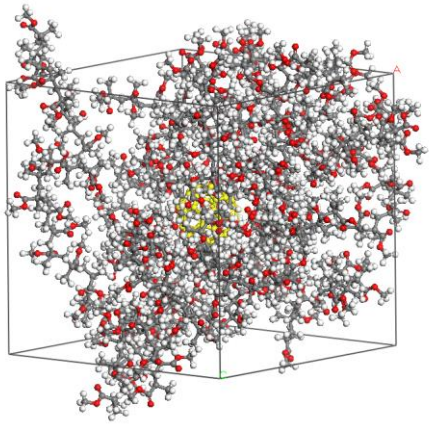

Fig. 5. Final configuration of the RVE with 3 wt.% of C_{60}.

Table 1. The initial and final characteristics of the RVEs with various concentration of C_{60} and $C_{60}@C_{240}$

Carbon filler	Percent of Concentration	Initial RVE Dimension (Å)	Final RVE Dimension (Å)	Initial density (g/cm^3)	Final density (g/cm^3)
C_{60}	0	36	31.20	0.70	1.096
C_{60}	1.02	100	47.34	0.12	1.109
C_{60}	2.01	50	37.65	0.48	1.114
C_{60}	3.03	45	32.80	0.43	1.117
C_{60}	4.06	40	29.71	0.46	1.124
$C_{60}@C_{240}$	5.02	70	47.17	0.35	1.135
$C_{60}@C_{240}$	10.09	50	37.06	0.47	1.163

3. Effective elastic constants

For linear elastic materials and using the Voigt matrix notation, the generalized Hooke's law is expressed as

$$\sigma_i = C_{ij}\varepsilon_j \tag{1}$$

where the coefficients C_{ij} are elastic constants, σ_i and ε_j are stress and strain components. Note that the stress is calculated from the virial stress formula. Therefore, the elastic constants can be determined by the partial derivatives of the virial stress components with respect to the strain components, i.e.,

$$C_{ij} = \frac{\partial \sigma_i}{\partial \varepsilon_j} \tag{2}$$

In addition, elastic compliance matrix S_{ij} is simply the matrix inverse of the elastic coefficients C_{ij}, i.e., $[S_{ij}] = [C_{ij}]^{-1}$. Since the nanofillers are symmetric and the PMMA molecules are dispersed randomly within the RVE, the effective macroscopic behaviour will be nearly isotropic and the material can be characterized by an effective Young's modulus and an effective Poisson's ratio. The effective elastic constants can be calculated by averaging the anisotropic elastic constants. The Voigt and the Reuss schemes are the most well-known averaging methods for estimating the effective elastic constants. According to the Voigt averaging method, Young's modulus (E_V) and Poisson's ratio (ν_V) are given by [16]

$$E_V = \frac{(A - B + 3C)(A + 2B)}{2A + 3B + C} \qquad \nu_V = \frac{A + 4B - 2C}{4A + 6B + 2C} \tag{3}$$

where

$$A = \frac{C_{11} + C_{22} + C_{33}}{3} \qquad B = \frac{C_{12} + C_{13} + C_{23}}{3} \qquad C = \frac{C_{44} + C_{55} + C_{66}}{3} \tag{4}$$

In addition, the Voigt bulk modulus (K_V) and shear modulus (G_V) are

$$K_V = \frac{A + 2B}{3} \qquad G_V = \frac{A - B + 3C}{5} \tag{5}$$

On the basis of the Reuss method, Young's modulus (E_R), Poisson's ratio (ν_R), bulk modulus (K_R) and shear modulus (G_R) are defined by

$$E_R = \frac{5}{3A' + 2B' + C'} \qquad \nu_R = -\frac{2A' + 8B' - C'}{6A' + 4B' + 2C'} \qquad K_R = \frac{1}{3(A' + 2B')} \qquad G_R = \frac{5}{4A' - 4B' + 3C'} \tag{6}$$

where

$$A' = \frac{S_{11} + S_{22} + S_{33}}{3} \qquad B' = \frac{S_{12} + S_{13} + S_{23}}{3} \qquad C' = \frac{S_{44} + S_{55} + S_{66}}{3} \tag{7}$$

In this study, we use the Voigt-Reuss-Hill approach which is good approximation to calculate the effective elastic constants. The effective Young's modulus and the effective Poisson's ratio are obtained by using the following relations.

$$E = \frac{E_V + E_R}{2} \qquad \nu = \frac{\nu_V + \nu_R}{2} \tag{8}$$

Mathematically, the elastic anisotropy can be described by using the universal anisotropic index A^U which is defined by [17]

$$A^U = 5\frac{G_V}{G_R} + \frac{K_V}{K_R} - 6 \tag{9}$$

It should be noted that A^U is identically zero for isotropic material and any variation from zero means anisotropic elastic properties.

4. Results and discussion

In this section, the elastic constants of the polymer composites reinforced with C_{60} fullerene and carbon onion are evaluated by using the MD simulation results and the Voigt-Reuss-Hill approach. Before determining the elastic constants, we study the distribution of polymer atoms around the fullerene in the RVE. Figure 6 shows the polymer density profile of the RVE with 2 wt.% of C_{60}.

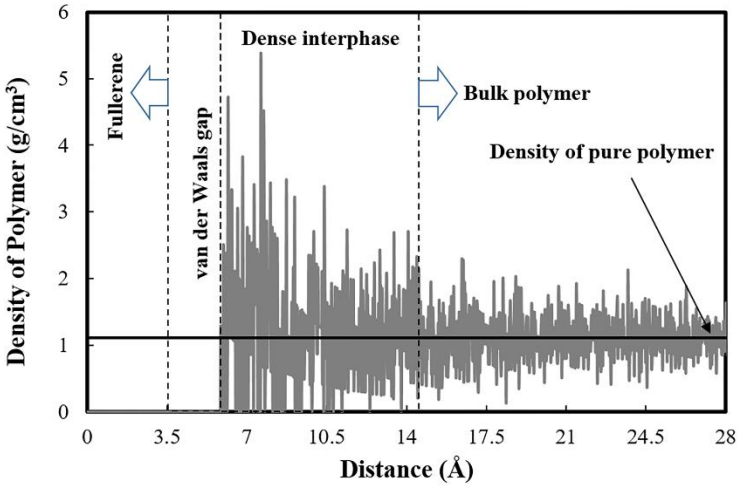

Fig. 6. Variations of the polymer density in the RVE with 2 wt.% of C_{60}

In this figure, the density of polymer is plotted against the distance measured from the fullerene center, r. It can be observed that the graph is divided into four regions. The first region, $r < 3.5$ Å, the polymer density is zero since there is no polymer in this region. The region between the external fullerene wall and inner surface of the polymer is known as "van der Waals gap". In this region, the density remains at zero. The van der Waals gap is depicted in Fig. 7.

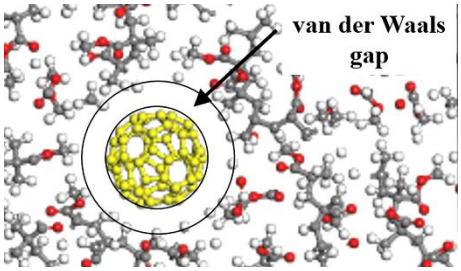

Fig. 7. Representation of the van de Waals gap

The third region, $6 < r < 15$ Å, is the adsorption layer interphase, which often has a greater density than the bulk polymer. This region is called a dense interphase [18, 19]. It has been shown that the existence of the dense interphase has a significant effect on the mechanical properties of the nanocomposites. The bulk polymer region is immediately after the dense interphase and this region has the same density of pure polymer.

Generally, the computed stiffness matrix of the RVE exhibits an anisotropic behavior. For example, the stiffness matrix for the RVE with 1 wt.% of C_{60} is

$$C = \begin{bmatrix} 4.3023 & 1.6879 & 1.6671 & 0.0835 & 0.0793 & 0.0559 \\ 1.6879 & 4.3934 & 1.4972 & 0.1129 & -0.0107 & -0.2288 \\ 1.6671 & 1.4972 & 4.2635 & -0.1082 & -0.0569 & -0.0533 \\ 0.0835 & 0.1129 & -0.1082 & 1.3362 & -0.0892 & 0.0021 \\ 0.0793 & -0.0107 & -0.0569 & -0.0892 & 1.1325 & -0.0347 \\ 0.0559 & -0.2288 & -0.0533 & 0.0021 & -0.0347 & 1.3209 \end{bmatrix} \text{(GPa)} \tag{10}$$

This result shows that the RVE is approximately isotropic and the stiffness matrix can be simplified as:

$$C = \begin{bmatrix} 4.3023 & 1.6879 & 1.6671 & 0 & 0 & 0 \\ 1.6879 & 4.3934 & 1.4972 & 0 & 0 & 0 \\ 1.6671 & 1.4972 & 4.2635 & 0 & 0 & 0 \\ 0 & 0 & 0 & 1.3362 & 0 & 0 \\ 0 & 0 & 0 & 0 & 1.1325 & 0 \\ 0 & 0 & 0 & 0 & 0 & 1.3209 \end{bmatrix} \text{(GPa)} \tag{11}$$

Using Eqs. (3)-(9), the elastic constants are determined. The computed values of the Young modulus and the Poisson ratio of C_{60}/PMMA and $C_{60}@C_{240}$/PMMA nanocomposites with various weight fractions are listed in Table 2. As expected, the Young modulus of the C_{60}/PMMA and $C_{60}@C_{240}$/PMMA composites increase when the weight fraction of the nano-fillers is increased. These results are consistent with the experimental observations. In addition, the results show that the Young modulus of the nanocomposite containing 10 wt.% of $C_{60}@C_{240}$ is close to that with 4 wt.% of C_{60}. This means that the presence of C_{60} molecule inside C_{240} has no significant influence on the Young modulus of nanocomposites. This can be explained by the fact that the van der Waals interactions between the C_{60} in the carbon onion and the polymer chains are very weak. In addition, calculated values of the universal anisotropic index are listed in Table 2. The results indicate that all RVEs exhibit nearly isotropic behaviour.

Table 2. Elastic properties of C_{60}/PMMA and $C_{60}@C_{240}$/PMMA nanocomposites with various weight fractions

Carbon filler	Percent of Concentration	G_V (GPa)	K_V (GPa)	G_R (GPa)	K_R (GPa)	E (GPa)	v	A^U
C_{60}	0	1.214	2.435	1.156	2.361	3.052	0.288	0.283
C_{60}	1.02	1.298	2.518	1.275	2.512	3.298	0.281	0.093
C_{60}	2.01	1.310	2.553	1.277	2.476	3.313	0.280	0.160
C_{60}	3.03	1.391	2.438	1.333	2.390	3.438	0.263	0.238
C_{60}	4.06	1.479	3.070	1.438	3.034	3.774	0.294	0.157
$C_{60}@C_{240}$	5.02	1.412	2.723	1.395	2.689	3.590	0.279	0.076
$C_{60}@C_{240}$	10.09	1.419	3.084	1.380	2.990	3.640	0.300	0.173

Finally, to confirm the validity of the MD simulations, we compare the computed results with some existing experimental results. The calculated ratios of Young' modulus of C_{60}/PMMA composites to Young's modulus of pure PMMA are shown in Fig. 8 along with the experimental data reported by Kropka et al. [20]. It can be seen that the results from the MD simulation are in reasonable agreement with the experimental results. As can be seen from this figure, the MD simulation results are higher than the experimental ones which may be due to the fact that the agglomeration occurs in experimental samples.

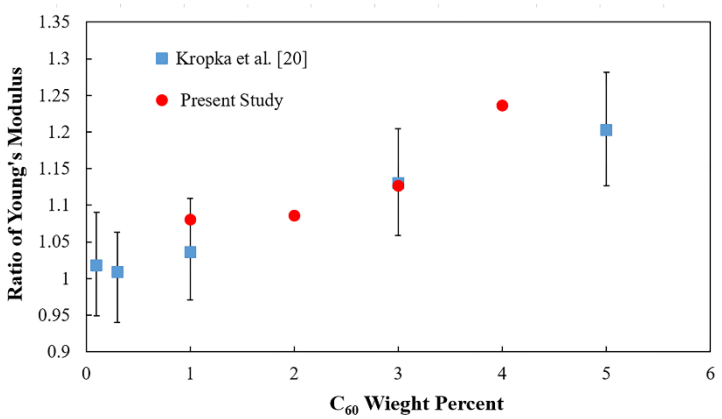

Fig. 8. Comparison between the results of present simulation and those given by Kropka et al. [20] for the ratio of Young's Modulus.

5. Conclusions

In this study, the MD simulations have been performed to study the elastic properties of spherical carbon nanofillers reinforced PMMA nanocomposites. To the best of our knowledge, this is the first time that the elastic properties of carbon onion reinforced polymer composites have been reported. The validity of the present simulations was successfully verified through comparison with available experimental data in the literature. Anisotropies of mechanical properties were studied by computing the universal anisotropic index. The results indicated that the elastic properties of the nanocomposites are nearly isotropic. The results indicated that the Young modulus of the nanocomposites increases with the increase of the filler weight fraction. Furthermore, it was observed that C_{60} molecule has better reinforcing capabilities than the $C_{60}@C_{240}$. The present study provides an insight on the elastic properties of C_{60}/PMMA and $C_{60}@C_{240}$/PMMA nanocomposites which are currently missing for subsequent static and dynamic modelling of the fullerene reinforced nanocomposite structures.

References

1. S.M. Rahimian-Koloor, S.M. Hashemianzadeh, M.M. Shokrieh, Effect of CNT structural defects on the mechanical properties of CNT/Epoxy nanocomposite, Physica B 540 (2018) 16-25.

2. A. Vahedi, M.H.S. Lahidjani, S. Shakhesi, Multiscale modeling of thermal conductivity of carbon nanotube epoxy nanocomposites, Physica B 550 (2018) 39-46.

3. T. Saotome, K. Kokubo, S. Shirakawa, T. Oshima, H.T. Hahn, Polymer nanocomposites reinforced with C_{60} fullerene: effect of hydroxylation, J. Compos. Mater. 45 (2011) 2595-2601.

4. A. Kausar, Carbon nano onion as versatile contender in polymer compositing and advance application, Fuller. Nanotub. Car. N. 25 (2017) 109-123.

5. C.T. Lu, A. Weerasinghe, D. Maroudas, A. Ramasubramaniam, A comparison of the elastic properties of graphene- and fullerene-reinforced polymer composites: the role of filler morphology and size, Sci. Rep. 6 (2016) 31735.

6. A. Adnan, C. Sun, H. Mahfuz, A molecular dynamics simulation study to investigate the effect of filler size on elastic properties of polymer nanocomposites, Compos. Sci. Technol. 67 (2007) 348-356.

7. S.F. Ferdous, M.F. Sarker, A. Adnan, Role of nanoparticle dispersion and filler-matrix interface on the matrix dominated failure of rigid C_{60}-PE nanocomposites: A molecular dynamics simulation study, Polymer 54 (2013) 2565-2576.

8. T. Ogasawara, Y. Ishida, T. Kasai, Mechanical properties of carbon fiber/fullerene-dispersed epoxy composites, Compos. Sci. Technol. 69 (2009) 2002-2007.

9. V.V. Zuev, S.V. Kostromin, A.V. Shlykov, The effect of fullerene fillers on the mechanical properties of polymer nanocomposites, Mech. Compos. Mater. 46 (2010) 147-154.

10. M. Hashemi Gahruei, Numerical characterisation of fullerene based polymer nanocomposites considering interface effects, Mater. Sci. Tech. 31 (2015) 1402-1407.

11. F. Jeyranpour, G. Alahyarizadeh, A. Minuchehr, The thermo-mechanical properties estimation of fullerene-reinforced resin epoxy composites by molecular dynamics simulation-A comparative study, Polymer 88 (2016) 9-18.

12. G.I. Giannopoulos, Linking MD and FEM to predict the mechanical behaviour of fullerene reinforced nylon-12, Compos. Part B 161 (2019) 455-463.

13. H. Sun, COMPASS: An ab initio force-field optimized for condensed-phase applications overview with details on alkane and benzene compounds, J. Phys. Chem. B 102 (1998) 7338-7364.

14. O.V. Alekseeva, A.V. Noskov, S.S. Guseynov, Features of the thermal behavior of PMMA/C_{60} film composites, Prot. Met. Phys. Chem. Surf. 52 (2016) 1019-1023.

15. D.N. Theodorou, U.W. Suter, Atomistic modeling of mechanical properties of polymeric glasses, Macromolecules 19 (1986) 139-154.

16. J.M.J. den Toonder, J.A.W. van Dommelen, F.P.T. Baaijens, The relation between single crystal elasticity and the effective elastic behaviour of polycrystalline materials: theory, measurement and computation, Model. Simul. Mater. Sc. Eng. 7 (1999) 909-928.

17. S.I. Ranganathan, M. Ostoja-Starzewski, Universal elastic anisotropy index, Phys. Rev. Lett. 101 (2008) 055504.

18. S. Herasati, L.C. Zhang, H.H. Ruan, A new method for characterizing the interphase regions of carbon nanotube composites, Int. J. Solids Struct. 51 (2014) 1781-1791.

19. S. Herasati, L.C. Zhang, Interphase effect on the macroscopic elastic properties of non-bonded single-walled carbon nanotube composites, Compos. Part B 77 (2015) 52-58.

20. J.M. Kropka, K.W. Putz, V. Pryamitsyn, V. Ganesan, P.F. Green, Origin of dynamical properties in PMMA-C_{60} nanocomposites, Macromolecules 40 (2007) 5424-5432.